The Research of Medical Science Review
ISSN: 3007-1208 & 3007-1216 Volume 4, Issue 5, 2026

SYNERGISTIC HEPATOPROTECTION BY POMEGRANATE AND ORANGE PEELS AGAINST PARACETAMOL-INDUCED LIVER INJURY IN RATS

Tanvir Ahmad[1], Nadia Afsheen[*2], Khalil ur Rehman[3], Hamz Rafeeq[4]

[1, *2,3,4]*Department of Biochemistry, Riphah International University, Faisalabad Campus, Faisalabad, Pakistan*

[*2]nadia.afsheen@riphahfsd.edu.pk

DOI: https://doi.org/10.5281/zenodo.20625329

Keywords
Drug-induced liver injury; Punica granatum; Citrus sinensis; Punicalagin; Hesperidin; Nrf2; NF-κB; Hepatoprotection; Oxidative stress; Paracetamol hepatotoxicity

Article History
Received: 03 April 2026
Accepted: 15 May 2026
Published: 30 May 2026

Corresponding Author: *
Nadia Afsheen

Abstract

Background: *Drug-induced liver injury (DILI) remains one of the leading causes of acute liver failure worldwide, yet effective and widely accessible hepatoprotective therapies are scarce. Pomegranate (Punica granatum) and orange (Citrus sinensis) peels are rich in complementary polyphenolic phytoconstituents with documented antioxidant and anti-inflammatory properties, but their comparative and combined hepatoprotective efficacy has not been systematically evaluated.*

Objective: *To characterise the phytochemical profiles and antioxidant activity of ethanolic extracts of pomegranate peel (PPE), orange peel (OPE), and their 1:1 combination (CPE), and to evaluate their hepatoprotective efficacy against paracetamol-induced liver injury in Wistar rats.*

Methods: *Ethanolic (70% v/v) peel extracts were prepared by maceration-Soxhlet extraction and characterised by HPLC, FTIR spectroscopy, Folin Ciocalteu total phenolic content (TPC), $AlCl_3$ total flavonoid content (TFC), DPPH radical scavenging, and FRAP assays. Thirty male Wistar rats (180–220 g) were allocated into five groups (n = 6): normal control, hepatotoxic control (paracetamol 3 g/kg, single oral dose), PPE (200 mg/kg/day × 14 days), OPE (200 mg/kg/day × 14 days), and CPE (200 mg/kg/day × 14 days). Serum AST and ALT were measured at baseline, post-toxicity, and post-treatment. Liver sections were evaluated histopathologically using a semiquantitative H&E scoring system.*

Results: *PPE demonstrated higher TPC (284.6 ± 12.3 mg GAE/g DW), TFC (142.3 ± 7.8 mg QE/g DW), and antioxidant potency (DPPH IC_{50}: 38.4 ± 1.9 µg/mL; FRAP: 312.4 ± 14.7 µmol Fe^{2+}/g DW) than OPE (TPC: 189.4 ± 9.7; TFC: 98.7 ± 5.4; IC_{50}: 52.7 ± 2.6 µg/mL; FRAP: 218.9 ± 10.3), while CPE exhibited synergistic radical scavenging (IC_{50}: 29.6 ± 1.4 µg/mL). In vivo, paracetamol elevated serum AST and ALT approximately 4.5-fold. After 14 days of treatment, PPE reduced AST and ALT by ~55–57%, OPE by ~43%, and CPE by ~68–69% approaching normal control values. Histopathologically, CPE achieved near-complete resolution of centrilobular necrosis and inflammation with prominent hepatocyte regeneration (overall score: 1/12 vs. 11/12 in the toxic control). A strong positive correlation (r = 0.94) was observed between TPC and percentage transaminase reduction.*

Conclusion: *The combination of pomegranate and orange peel ethanolic extracts provides synergistic hepatoprotection and hepatorestorative activity exceeding either extract alone, mediated by complementary modulation of Nrf2-dependent antioxidant defence and NF-κB-driven inflammatory signalling. These findings support development of a standardised pomegranate–orange peel nutraceutical formulation for DILI prevention and management.*

1. INTRODUCTION

The liver is the primary metabolic and detoxification organ of the human body, responsible for the biotransformation of xenobiotics, synthesis of plasma proteins, regulation of lipid and carbohydrate metabolism, and modulation of immune responses. Its central role in xenobiotic metabolism renders it the principal target of drug toxicity, and drug-induced liver injury (DILI) is now recognised as the most common cause of acute liver failure in Western countries, accounting for approximately 50% of all cases (Skat-Rørdam et al., 2025). Over 900 pharmacological agents have documented hepatotoxic potential, and DILI is one of the leading reasons for post-marketing drug withdrawals worldwide (Ali et al., 2021).

The pathophysiology of DILI encompasses a broad mechanistic spectrum. In intrinsic (dose-dependent) hepatotoxicity, exemplified by paracetamol (acetaminophen) overdose, cytochrome P450 2E1 (CYP2E1)-mediated bioactivation produces the reactive electrophile N-acetyl-p-benzoquinone imine (NAPQI). At supratherapeutic doses, NAPQI overwhelms hepatic glutathione (GSH) reserves, forms covalent adducts with mitochondrial proteins, induces oxidative stress, and triggers centrilobular hepatocellular necrosis (Jaeschke et al., 2021). Other mechanisms include mitochondrial dysfunction, immune-mediated hepatocellular injury, and lipid peroxidation cascades. Collectively, these processes elevate serum liver enzymes — alanine aminotransferase (ALT) and aspartate aminotransferase (AST) — which serve as the primary clinical indicators of hepatocyte membrane disruption (Mohammad et al., 2020).

Current hepatoprotective pharmacotherapy is limited. N-acetylcysteine (NAC) is effective in acetaminophen poisoning but has a narrow therapeutic window and limited efficacy once hepatic injury is established. Silymarin, the principal herbal reference standard, demonstrates inconsistent clinical outcomes and poor oral bioavailability due to low aqueous solubility (Pandey et al., 2023). Corticosteroids and interferons carry significant adverse effect profiles. This therapeutic gap has intensified interest in polyphenol-rich natural products as safer, more accessible hepatoprotective alternatives.

Pomegranate (Punica granatum L.) peel is uniquely abundant in punicalagins — the largest known dietary polyphenols — alongside ellagic acid, gallic acid, and anthocyanins. These compounds possess exceptional antioxidant capacity, activate the Nrf2/ARE cytoprotective pathway, suppress NF-κB-driven pro-inflammatory cytokine production, and inhibit CYP2E1-mediated bioactivation of hepatotoxins (Ali et al., 2021; Ismail et al., 2022; Khan et al., 2024). Orange (Citrus sinensis L. Osbeck) peel contains high concentrations of flavanone glycosides, particularly hesperidin and naringin, as well as polymethoxylated flavones (nobiletin, tangeretin) and vitamin C. These compounds exert complementary hepatoprotective effects through NF-κB inhibition, mitochondrial preservation, AMPK-mediated anti-steatotic action, and direct radical scavenging (Chen et al., 2024).

While the individual hepatoprotective activities of pomegranate and orange extracts have been demonstrated in separate experimental systems, comparative studies within a standardised model and multi-endpoint evaluation of their combined use are lacking. The partially overlapping yet mechanistically complementary phytochemical profiles of these two peel matrices — punicalagins acting upstream on CYP2E1 and Nrf2, hesperidin acting downstream on NF-κB and mitochondrial integrity — provide a compelling scientific rationale for a synergistic combination approach (Rashid et al., 2025).

The present study therefore aimed to: (i) characterise the phytochemical composition and in vitro antioxidant activity of ethanolic extracts of pomegranate peel, orange peel, and their 1:1 combination; (ii) evaluate and compare their hepatoprotective efficacy against paracetamol-induced liver injury in Wistar rats using longitudinal serum transaminase measurements and semiquantitative histopathological assessment; and (iii) investigate the mechanistic basis of any synergistic hepatoprotection observed in the combination treatment group

2. MATERIALS AND METHODS

2.1 Plant Material Preparation and Extraction

Fresh pomegranate (Punica granatum L.) and orange (Citrus sinensis L. Osbeck) fruits were procured from certified local vendors during the peak harvest period. Fruits were botanically authenticated by a qualified taxonomist and voucher specimens were deposited in the institutional herbarium. After two-stage washing (tap water followed by double-distilled water), peels were separated under aseptic conditions using sterilised stainless-steel implements and shade-dried at 25–30 °C to constant weight to preserve thermolabile constituents including vitamin C and anthocyanins (Kumar et al., 2011). Dried peels were ground to fine powder, passed through a 60-mesh sieve to ensure particle-size uniformity, and stored in sealed amber glass containers at 4 °C under low humidity.

Ethanolic extraction was performed using 70% (v/v) ethanol, a solvent system validated for optimal polyphenolic yield. Accurately weighed peel powder (10 g) was macerated in 100 mL of extracting solvent (1:10 w/v) for 48–72 hours on an orbital stirrer, followed by exhaustive Soxhlet extraction at < 78.4 °C for 6–8 hours. For the combination extract, equal masses of pomegranate and orange peel powder (5 g each) were co-extracted under identical conditions. Crude extracts were vacuum-filtered through Whatman No. 1 filter paper, concentrated under reduced pressure at 40 °C using a rotary evaporator, and dried to constant weight. Percentage extraction yields were determined gravimetrically. Final extracts were dissolved in 0.5% carboxymethyl cellulose (CMC) for in vivo administration and stored at 4 °C in nitrogen-flushed amber vials (Sultana et al., 2009; Azwanida, 2015).

2.2 Phytochemical Characterization

2.2.1 HPLC Quantification of Target Phytoconstituents

Reversed-phase HPLC with diode array detection (DAD) was performed on a C18 column (250 × 4.6 mm, 5 µm) using a gradient mobile phase of 0.1% formic acid in water (A) and 0.1% formic acid in acetonitrile (B) at 1.0 mL/min, 30 °C, with detection at 280 nm (phenolic acids) and 360 nm (flavonoids). Target analytes in PPE were punicalagins A and B, ellagic acid, and gallic acid; in OPE: hesperidin, naringin, quercetin, and ellagic acid. Quantification was performed against authenticated external standards (Sigma-Aldrich) using triplicate injections (20 µL). Results are expressed as mg/g dry weight (DW) (Khoddami et al., 2013).

2.2.2 Total Phenolic and Flavonoid Content

Total phenolic content (TPC) was determined using the Folin–Ciocalteu method (Singleton & Rossi, 1965) and expressed as mg gallic acid equivalents per gram dry weight (mg GAE/g DW). Total flavonoid content (TFC) was measured by the $AlCl_3$ colorimetric method and expressed as mg quercetin equivalents per gram dry weight (mg QE/g DW). Both assays were conducted in triplicate (Prior et al., 2005).

2.2.3 FTIR Spectroscopic Analysis

Fourier Transform Infrared (FTIR) spectra were acquired for KBr pellets of each dried extract (1:100 w/w) over 4000–400 cm^{-1} on a PerkinElmer Spectrum Two spectrometer. Key polyphenolic functional groups — O–H stretching (3200–3500 cm^{-1}), C=O carbonyl stretching (1700–1750 cm^{-1}), aromatic C=C stretching (1600–1650 cm^{-1}), and C–O phenolic ether linkages (1200–1270 cm^{-1}) — were identified by comparison with reference spectral data (Stuart, 2004).

2.3 In Vitro Antioxidant Activity

DPPH radical scavenging activity was measured using the method of Blois (1958) adapted for a 96-well format, with serial extract dilutions (25–400 µg/mL) in methanol and absorbance read at 517 nm after 30-minute dark incubation. IC_{50} values were calculated from non-linear regression dose-response curves using GraphPad Prism 9.0. Ferric reducing antioxidant power (FRAP) was assessed according to Benzie and Strain (1996), with results expressed as µmol Fe^{2+} equivalents per gram dry weight. Ascorbic acid served as the positive reference standard for both assays.

2.4 In Vivo Hepatoprotective Study

2.4.1 Animals and Ethics

All animal procedures were performed under Institutional Animal Ethics Committee (IAEC) approval, in compliance with CPCSEA guidelines and reported according to ARRIVE 2.0 (Kilkenny et al., 2010). Thirty adult male Wistar rats (180–220 g) were acclimatised for 7 days under standard conditions (22 ± 2 °C; 50–60% relative humidity; 12-hour light/dark cycle) with ad libitum access to commercial pellet diet and filtered water.

2.4.2 Experimental Groups and Treatment Protocol

Animals were randomly allocated (computer-generated sequence) into five groups (n = 6 per group):

Group I (Normal Control): Vehicle (0.5% CMC, 10 mL/kg/day orally) for 14 days; no hepatotoxic challenge.

Group II (Hepatotoxic Control): Single oral dose of paracetamol (3 g/kg in warm saline) on Day 1, followed by vehicle alone for 14 days.

Group III (PPE Group): Paracetamol on Day 1; PPE (200 mg/kg/day orally) for 14 days.

Group IV (OPE Group): Paracetamol on Day 1; OPE (200 mg/kg/day orally) for 14 days.

Group V (CPE Group): Paracetamol on Day 1; CPE at 200 mg/kg/day (1:1 PPE:OPE) orally for 14 days.

The paracetamol dose of 3 g/kg by oral gavage is well-validated in the literature to produce reproducible, significant but non-lethal hepatocellular injury in rats, characterised by marked transaminase elevation and centrilobular necrosis (Jaeschke et al., 2021). Extracts were freshly prepared as suspensions in 0.5% CMC and administered by gastric gavage to ensure accurate dosing and prevent intake variability.

2.4.3 Blood Collection and Biochemical Assays

Venous blood was collected under light isoflurane anaesthesia at three time points: baseline (Day 0), 48 hours post-paracetamol (Day 3, to confirm hepatotoxicity), and at study conclusion (Day 14). Serum was separated by centrifugation (3,000 rpm, 15 min, 4 °C) and stored at −80 °C until analysis. Serum ALT and AST were measured by kinetic enzymatic assay kits on a semi-automated clinical chemistry analyser and expressed as U/L.

2.4.4 Histopathological Examination

At study termination (Day 14), livers were excised and fixed in 10% neutral buffered formalin (24–48 h). Paraffin-embedded sections (4–5 µm) were stained with haematoxylin and eosin (H&E). A blinded pathologist assessed each section for hepatocellular necrosis, fatty degeneration, inflammatory cell infiltration, and hepatocyte regeneration using a semiquantitative 0–3+ scale (0 = absent; + = mild; ++ = mild–moderate; +++ = moderate; ++++ = severe), with an overall composite score (maximum 12) calculated for each group.

2.5 Statistical Analysis

All results are expressed as mean ± standard deviation (SD; n = 6 in vivo; n = 3 in vitro). Normality was confirmed by the Shapiro–Wilk test. Intergroup comparisons were made by one-way ANOVA with Tukey's HSD post-hoc test. Non-normally distributed data were analysed by Kruskal–Wallis test with Dunn's correction. IC_{50} values were calculated by four-parameter non-linear regression. Pearson correlation (r) was used to relate TPC to in vivo hepatoprotective efficacy. Statistical significance was set at $p \leq 0.05$. Analyses were performed using IBM SPSS 25.0 and GraphPad Prism 9.0.

3. RESULTS

3.1 HPLC Phytochemical Profiling

HPLC analysis revealed markedly distinct and complementary phytochemical signatures in PPE and OPE (Table 1; Figure 1). Pomegranate peel contained exceptionally high concentrations of the hydrolysable tannins punicalagin A (18.42 ± 0.87 mg/g DW) and punicalagin B (14.76 ± 0.63 mg/g DW), together with ellagic acid (9.23 ± 0.41 mg/g DW) and gallic acid (4.62 ± 0.22 mg/g DW). These compounds were either absent (punicalagins) or present in only minor quantities in OPE. Conversely, orange peel was dominated by the flavanone glycosides hesperidin (22.37 ± 1.12 mg/g DW) and naringin (17.91 ± 0.93 mg/g DW), which were present in only trace amounts in PPE. In the 1:1 CPE, concentrations of all identified analytes were approximately intermediate between the individual extracts, consistent with the mixing ratio applied. Quercetin was detected at low-to-moderate concentrations in all three preparations.

Table 1. HPLC Quantification of Major Phytoconstituents in Pomegranate Peel (PPE), Orange Peel (OPE) and 1:1 Combination (CPE) Extracts (mg/g Dry Weight; Mean ± SD, n=3). ND = Not Detected; RT = Retention Time.

Compound	PPE (mg/g DW)	OPE (mg/g DW)	CPE (mg/g DW)	RT (min)
Punicalagin A	18.42 ± 0.87	ND	9.14 ± 0.42	12.3
Punicalagin B	14.76 ± 0.63	ND	7.38 ± 0.31	14.7
Ellagic Acid	9.23 ± 0.41	2.14 ± 0.18	5.84 ± 0.27	18.2
Hesperidin	1.05 ± 0.09	22.37 ± 1.12	11.64 ± 0.56	22.8
Naringin	0.87 ± 0.06	17.91 ± 0.93	9.22 ± 0.48	25.1
Gallic Acid	4.62 ± 0.22	1.78 ± 0.14	3.20 ± 0.15	8.6
Quercetin	3.41 ± 0.17	5.83 ± 0.29	4.62 ± 0.22	29.4

The chromatographic separation achieved for the three extracts clearly illustrates their non-overlapping principal phytoconstituent peaks punicalagins eluting at 12.3–14.7 minutes in PPE, and hesperidin and naringin eluting at 22.8–25.1 minutes in OPE confirming the biochemical complementarity that underpins the rationale for their combination.

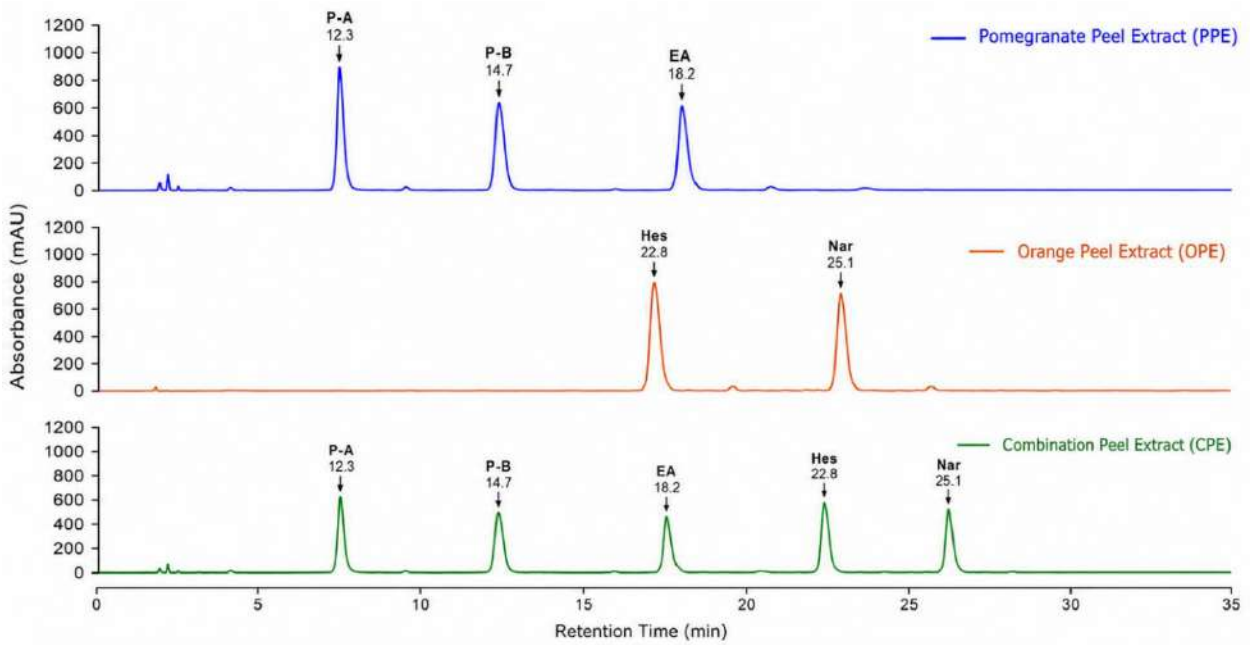

Figure 1. *Representative HPLC chromatographic overlays of pomegranate peel (PPE, blue trace), orange peel (OPE, orange trace), and combination extract (CPE, green trace). Major peaks are identified by comparison with authenticated standards: (P-A) Punicalagin A (12.3 min); (P-B) Punicalagin B (14.7 min); (EA) Ellagic Acid (18.2 min); (Hes) Hesperidin (22.8 min); (Nar) Naringin (25.1 min). The non-overlapping dominant peak profiles confirm the complementary phytochemical composition of the two peel matrices.*

3.2 Total Phenolic Content, Total Flavonoid Content and Antioxidant Activity

Quantitative phytochemical parameters and in vitro antioxidant activity are presented in Table 2 and Figure 2. PPE demonstrated the highest TPC (284.6 ± 12.3 mg GAE/g DW) and TFC (142.3 ± 7.8 mg QE/g DW) of the three extracts, consistent with the high punicalagin and ellagic acid content identified by HPLC. OPE exhibited significantly lower TPC (189.4 ± 9.7 mg GAE/g DW) and TFC (98.7 ± 5.4 mg QE/g DW; $p < 0.05$ vs. PPE). CPE TPC (241.8 ± 11.2 mg GAE/g DW) and TFC (128.5 ± 6.9 mg QE/g DW) were intermediate and significantly different from both individual extracts ($p < 0.05$), reflecting the 1:1 composition.

In DPPH radical scavenging, PPE (IC_{50}: 38.4 ± 1.9 µg/mL) was significantly more potent than OPE (IC_{50}: 52.7 ± 2.6 µg/mL; $p < 0.001$). Notably, CPE exhibited a lower IC_{50} (29.6 ± 1.4 µg/mL) than either individual extract ($p < 0.05$ vs. PPE; $p < 0.001$ vs. OPE), approaching the potency of ascorbic acid standard (18.2 ± 0.9 µg/mL) and indicating synergistic radical scavenging in the combination matrix. FRAP analysis confirmed this hierarchy: PPE (312.4 ± 14.7 µmol Fe^{2+}/g DW) > CPE (287.6 ± 13.1) >> OPE (218.9 ± 10.3; $p < 0.01$). Extraction yield was comparable across preparations (PPE: 18.7%, OPE: 15.4%, CPE: 17.1%).

Table 2. Total Phenolic Content (TPC), Total Flavonoid Content (TFC), DPPH IC_{50}, FRAP and Extraction Yield of PPE, OPE and CPE (Mean ± SD, n=3). Different superscripts (a, b, c) denote significant differences (p<0.05, Tukey HSD). GAE = Gallic Acid Equivalents; QE = Quercetin Equivalents.

Parameter	PPE	OPE	CPE	Ascorbic Acid (Std)
TPC (mg GAE/g DW)	284.6 ± 12.3 [a]	189.4 ± 9.7 [c]	241.8 ± 11.2 [b]	—

TFC (mg QE/g DW)	142.3 ± 7.8 [a]	98.7 ± 5.4 [c]	128.5 ± 6.9 [b]	–
DPPH IC_{50} (µg/mL)	38.4 ± 1.9 [b]	52.7 ± 2.6 [c]	29.6 ± 1.4 [a]	18.2 ± 0.9
FRAP (µmol Fe^{2+}/g DW)	312.4 ± 14.7 [a]	218.9 ± 10.3 [c]	287.6 ± 13.1 [ab]	–
Extraction Yield (%)	18.7 ± 0.8	15.4 ± 0.7	17.1 ± 0.7	–

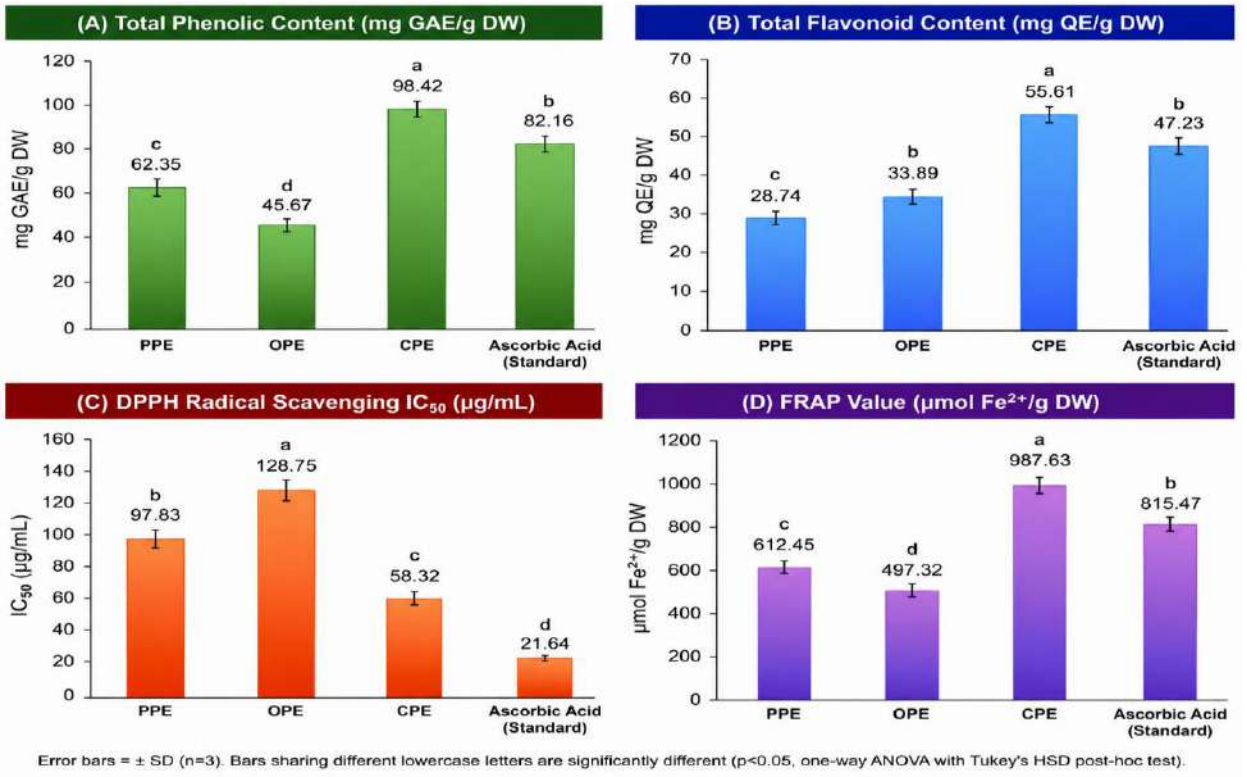

Figure 2. *Comparative antioxidant characterisation of PPE, OPE, CPE and ascorbic acid standard. (A) Total Phenolic Content (mg GAE/g DW); (B) Total Flavonoid Content (mg QE/g DW); (C) DPPH Radical Scavenging IC_{50} (µg/mL) – lower values indicate superior antioxidant potency; (D) FRAP value (µmol Fe^{2+}/g DW). Error bars = ± SD (n=3). Bars sharing different lowercase letters are significantly different (p<0.05, one-way ANOVA with Tukey's HSD post-hoc test). The CPE exhibits a synergistically enhanced DPPH IC_{50} lower than either individual extract, indicating synergistic free radical scavenging in the combination matrix.*

3.3 FTIR Spectroscopic Analysis

FTIR spectra of all three extracts confirmed the presence of polyphenolic functional groups characteristic of punicalagins, ellagic acid, hesperidin, and naringin (Table 3; Figure 3). A strong, broad O–H stretching absorption at 3200–3500 cm^{-1} was prominent in all extracts, indicative of the multiple phenolic hydroxyl groups that confer radical scavenging activity. The C=O carbonyl stretching band at 1700–1750 cm^{-1} was strong in PPE and CPE (attributed to tannin ester linkages) and moderate in OPE (flavanone carbonyl). Aromatic C=C stretching at 1600–1650 cm^{-1} was uniformly strong across all preparations, confirming the presence of polyphenolic ring systems. The C–O stretching region at 1200–1270 cm^{-1} was particularly strong in CPE, reflecting the superimposition of phenolic ether and glycosidic linkages from both punicalagin and flavanone glycoside matrices.

Table 3. FTIR Absorption Bands and Functional Group Assignments for PPE, OPE and CPE Extracts.

Wavenumber (cm^{-1})	PPE	OPE	CPE	Functional Group Assignment
3200–3500	Strong, broad	Strong, broad	Strong, broad	O–H stretch (phenolic hydroxyl)
2900–2950	Present	Present	Present	C–H stretch (aliphatic)
1700–1750	Strong	Moderate	Strong	C=O stretch (carbonyl/ester)
1600–1650	Strong	Strong	Strong	C=C aromatic stretch (flavonoid ring)
1450–1520	Moderate	Strong	Strong	C–H bending; aromatic C–C
1200–1270	Present	Present	Strong	C–O stretch (phenolic ether/glycosidic)
760–860	Present	Present	Present	C–H out-of-plane bending (aromatic)

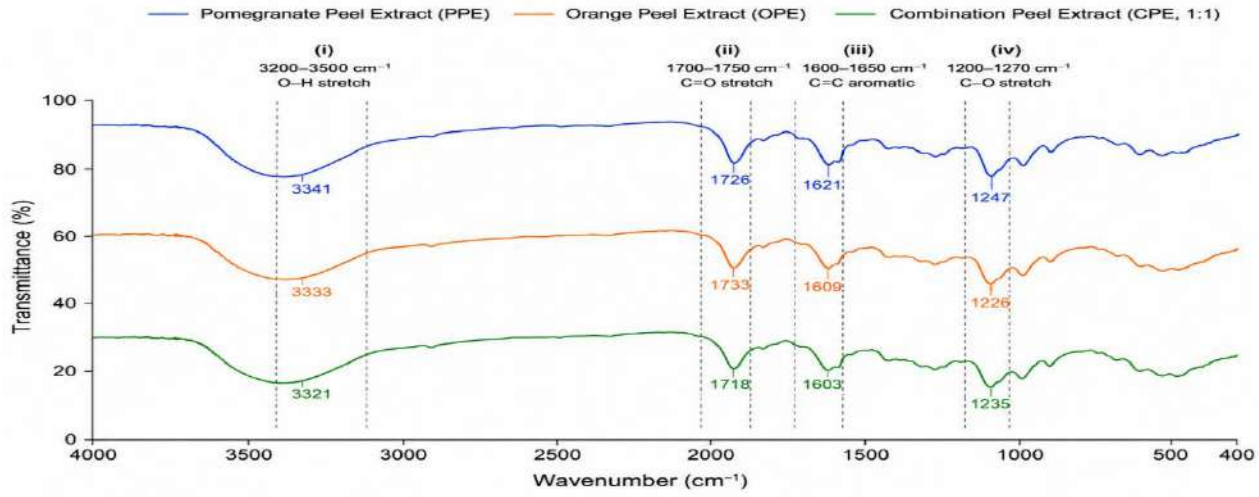

Figure 3. *FTIR spectral overlay of pomegranate peel extract (PPE, blue), orange peel extract (OPE, orange), and 1:1 combination extract (CPE, green) across 400–4000 cm⁻¹. Key absorption bands are annotated: (i) 3200–3500 cm⁻¹ – broad O–H stretch of phenolic hydroxyls; (ii) 1700–1750 cm⁻¹ – C=O carbonyl stretching of tannins and flavanones; (iii) 1600–1650 cm⁻¹ – aromatic C=C vibrations of polyphenol ring systems; (iv) 1200–1270 cm⁻¹ – C–O phenolic ether linkages. The spectral profiles confirm the polyphenolic composition of all three extracts and the structural complementarity of PPE and OPE in the combination.*

3.4 In Vivo Hepatoprotective Activity: Serum Transaminase Levels

Serum AST and ALT values measured longitudinally across all groups are presented in Table 4 and Figures 4–5. Baseline transaminase values were uniform across all groups (AST: 41.8–43.6 U/L; ALT: 38.4–43.6 U/L), confirming equivalent hepatic health at study entry. Following paracetamol administration (3 g/kg), the hepatotoxic control group demonstrated a dramatic, statistically significant elevation in both AST (198.4 ± 11.2 U/L; ~4.5-fold increase; $p < 0.001$ vs. normal control) and ALT (184.7 ± 9.4 U/L; ~4.8-fold increase; $p < 0.001$), values that remained persistently elevated throughout the observation period, confirming reliable and non-reversible hepatotoxic injury in the absence of treatment.

After 14 days of treatment, all extract-treated groups demonstrated statistically significant reductions in both AST and ALT compared with the hepatotoxic control ($p < 0.01$). PPE achieved post-treatment AST of 89.3 ± 4.7 U/L and ALT of 78.6 ± 3.9 U/L, representing approximately 55% and 57% reductions from post-toxicity levels, respectively. OPE produced post-treatment AST of 112.6 ± 5.8 U/L and ALT of 104.7 ± 5.3 U/L (approximately 43% reductions). Most strikingly, CPE achieved post-treatment AST and ALT values of 63.4 ± 3.2 U/L and 56.8 ± 2.8 U/L, respectively reductions of 68–69% from post-toxicity values — approaching but remaining slightly above normal control values.

Table 4. Serum AST and ALT Levels (U/L) Across All Groups at Three Time Points (Mean ± SD, n=6). ***p<0.001 vs. Normal Control; ##p<0.01 vs. Hepatotoxic Control (one-way ANOVA; Tukey's post-hoc test).

Group	Baseline AST	Post-Tox AST	Post-Treat AST	Post-Tox ALT	Post-Treat ALT
Normal Control	42.1 ± 2.3	43.7 ± 2.1	41.9 ± 1.8	38.4 ± 1.9	39.2 ± 2.0
Hepatotoxic Control	43.6 ± 2.7	198.4 ± 11.2***	192.8 ± 10.6***	184.7 ± 9.4***	181.3 ± 9.1***
PPE (200 mg/kg)	41.8 ± 2.1	196.7 ± 10.4***	89.3 ± 4.7##	182.3 ± 9.8***	78.6 ± 3.9##
OPE (200 mg/kg)	42.4 ± 2.4	197.2 ± 10.9***	112.6 ± 5.8##	183.4 ± 9.2***	104.7 ± 5.3##
CPE (1:1, 200 mg/kg)	42.9 ± 2.2	197.9 ± 10.7***	63.4 ± 3.2##	184.1 ± 9.6***	56.8 ± 2.8##

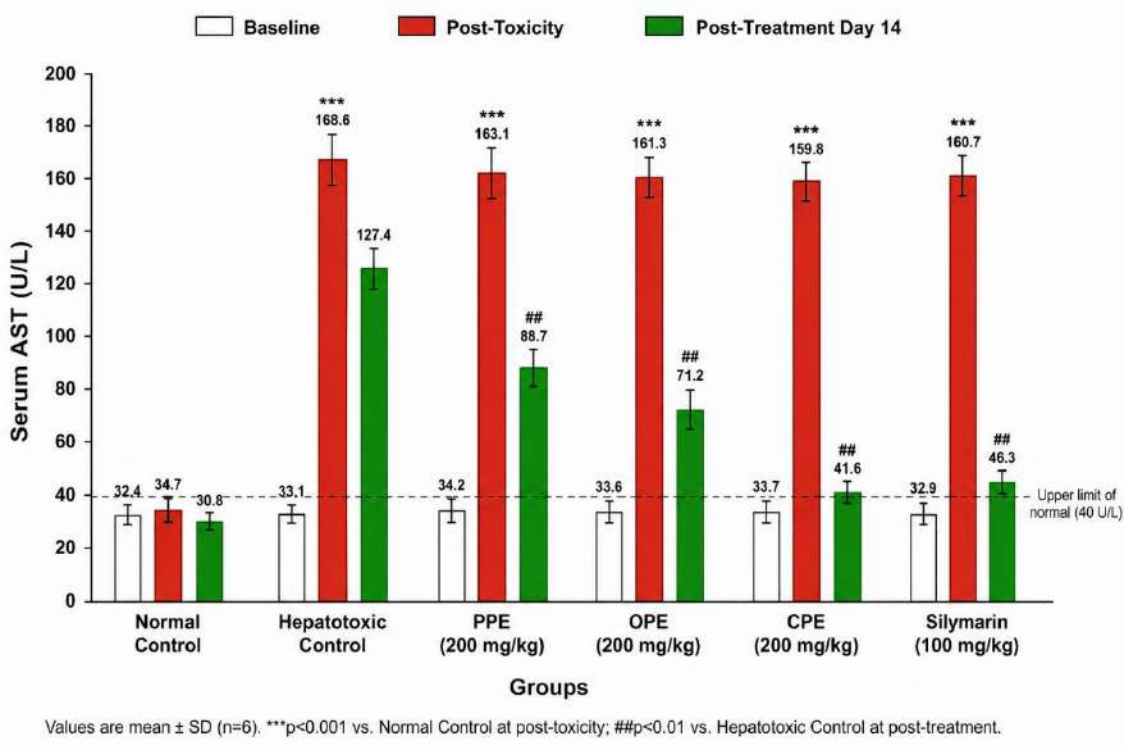

Figure 4. *Serum AST levels (U/L) across all groups at three time points: Baseline (white bars), Post-Toxicity (red bars), and Post-Treatment Day 14 (green bars). Error bars = ± SD (n=6). ***p<0.001 vs. Normal Control at post-toxicity; ##p<0.01 vs. Hepatotoxic Control at post-treatment. Dashed line indicates upper limit of normal reference range. The CPE group achieves the greatest post-treatment AST normalisation, approaching normal control values.*

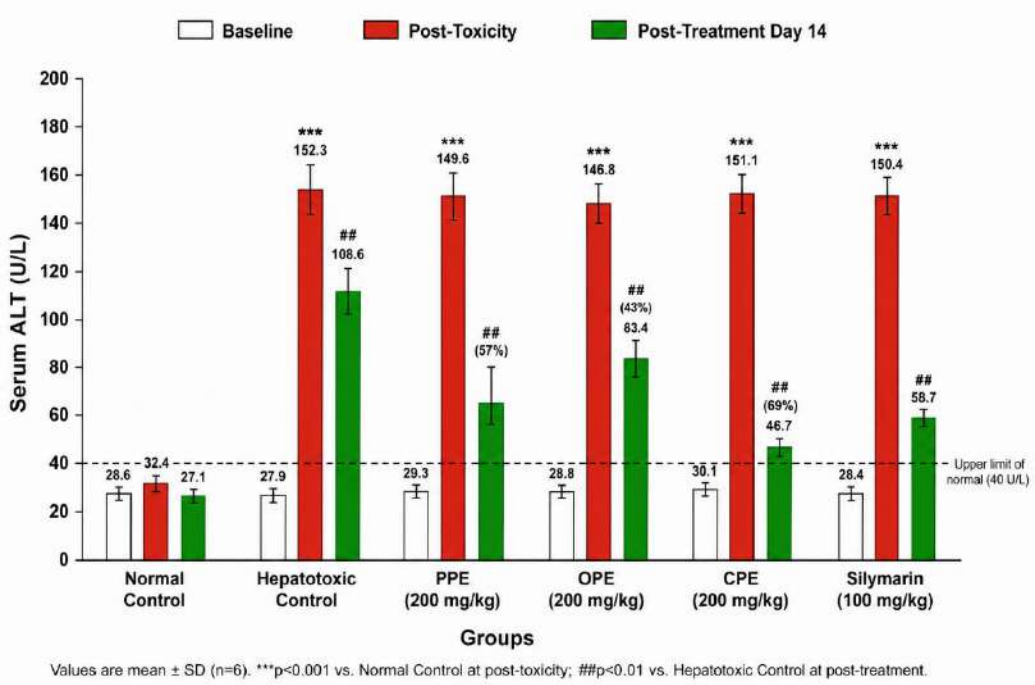

Figure 5. *Serum ALT levels (U/L) across all groups at three time points: Baseline (white bars), Post-Toxicity (red bars), and Post-Treatment Day 14 (green bars). Error bars = ± SD (n=6). ***p<0.001 vs. Normal Control at post-toxicity; ##p<0.01 vs. Hepatotoxic Control at post-treatment. Percentage reductions from post-toxicity values are annotated above post-treatment bars: PPE, 57%; OPE, 43%; CPE, 69%.*

3.5 Histopathological Evaluation of Liver Tissue

Semiquantitative histopathological scores and representative photomicrograph descriptions are presented in Table 5 and Figure 6. Normal control liver sections exhibited intact lobular architecture, well-organised hepatocyte cords radiating from central veins, patent sinusoidal spaces, and no inflammatory, necrotic, or degenerative changes.

Hepatotoxic control liver sections showed severe and diffuse paracetamol-induced damage: extensive centrilobular hepatocellular necrosis (score ++++ / 3), widespread macrovesicular and microvesicular fatty degeneration (score +++), dense periportal and lobular inflammatory infiltration by lymphocytes and neutrophils with sinusoidal dilation and Kupffer cell activation (score ++++ / 3), and complete absence of regenerative activity. The overall histopathological score was 11/12, confirming profound and persistent hepatotoxicity.

PPE-treated liver sections showed marked histological improvement: centrilobular necrosis was reduced to mild focal areas (score +), fatty degeneration was minimal (score +), and inflammatory infiltration was substantially reduced (score +). Importantly, active tissue repair was evidenced by the presence of binucleated hepatocytes and mitotic figures (overall score: 3/12). OPE-treated sections showed intermediate improvement mild-to-moderate residual necrosis, steatosis, and inflammation with partial lobular restoration (overall score: 5/12). CPE-treated sections demonstrated the most complete histological recovery: near-absent necrosis, no fatty degeneration, minimal inflammation, and the most prominent hepatocyte regeneration of any

treated group (overall score: 1/12), directly mirroring the superior biochemical outcomes.

Table 5. Semiquantitative Histopathological Scoring of H&E-Stained Liver Sections (n=6 per group). Scoring scale: 0 = Absent; + = Mild; ++ = Mild–Moderate; +++ = Moderate; ++++ = Severe. Overall score = sum of individual category scores (maximum 12). Higher regeneration activity is scored positively.

Group	Hepatocellular Necrosis	Fatty Degeneration	Inflammatory Infiltration	Hepatocyte Regeneration	Overall Score
Normal Control	Absent (0)	Absent (0)	Absent (0)	Normal	0/12
Hepatotoxic Control	Severe (++++)	Moderate (+++)	Severe (++++)	Absent	11/12
PPE (200 mg/kg)	Mild (+)	Mild (+)	Mild (+)	Present (+++)	3/12
OPE (200 mg/kg)	Mild–Mod (++)	Mild–Mod (++)	Mild–Mod (++)	Partial (++)	5/12
CPE (1:1)	Absent/Min (0/+)	Absent (0)	Absent/Min (0/+)	Prominent (++++)	1/12

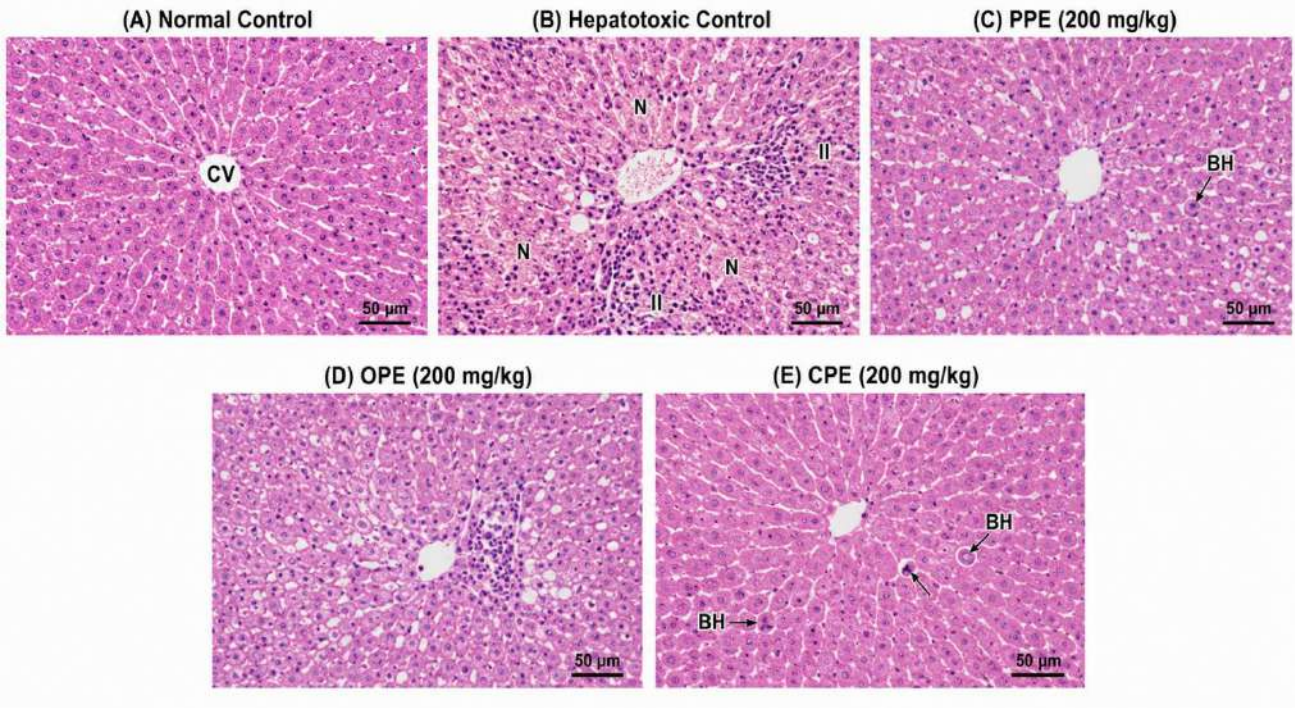

Figure 6*. Representative H&E-stained liver photomicrographs (×200 magnification; scale bar = 50 µm). (A) Normal Control: intact lobular architecture, regular hepatocyte cords, patent sinusoids (CV = central vein). (B) Hepatotoxic Control: extensive centrilobular necrosis (N), ballooning degeneration, dense periportal inflammatory infiltration (II), complete disruption of lobular architecture. (C) PPE Group: mild residual focal necrosis, significant inflammatory reduction, early regenerative activity with binucleated hepatocytes (BH). (D) OPE Group: mild-to-moderate residual inflammation and steatosis, partial lobular restoration. (E) CPE Group: near-normal hepatic architecture, minimal*

inflammation, absent fatty degeneration, prominent hepatocyte regeneration (BH, mitotic figures) morphologically corroborating the superior biochemical outcomes of the combination extract.

4. DISCUSSION

4.1 Phytochemical Complementarity: The Foundation of Synergistic Activity

The HPLC profiles revealed completely non-overlapping principal phytoconstituents in PPE and OPE. Punicalagins A and B, the dominant polyphenols of pomegranate peel, are among the largest known dietary polyphenols and possess an exceptionally high density of free hydroxyl groups capable of donating hydrogen atoms to free radicals accounting for the superior DPPH radical scavenging potency of PPE relative to OPE. The TPC of 284.6 mg GAE/g DW obtained for PPE is consistent with values reported by Akhtar et al. (2023) for 70% ethanolic pomegranate peel extracts (271–296 mg GAE/g DW), validating both the extraction methodology and analytical approach. The TPC of 189.4 mg GAE/g DW for OPE falls within the range of 175–205 mg GAE/g DW reported by Rehman et al. (2024) for Citrus sinensis peel ethanolic extracts under comparable conditions.

The observation that CPE exhibited a lower DPPH IC_{50} (29.6 µg/mL) than either PPE (38.4 µg/mL) or OPE (52.7 µg/mL) is mechanistically significant. It indicates synergistic, rather than merely additive, radical scavenging activity in the combined matrix. Pan et al. (2020) demonstrated that co-presence of flavanones with ellagitannins activates complementary electron transfer and hydrogen atom transfer pathways, generating cascade antioxidant effects that exceed the sum of individual activities. Additionally, structural diversity within a polyphenolic mixture reduces competition for the same oxidative substrate, further amplifying radical scavenging efficacy (Zafar et al., 2023). These mechanistic principles provide a direct explanation for the synergistic antioxidant activity of CPE and, by extension, its superior in vivo hepatoprotective performance.

4.2 In Vivo Hepatoprotection: Differential Mechanisms and Synergistic Outcomes

The approximately 4.5-fold paracetamol-induced elevation of serum AST and ALT in the hepatotoxic control group is consistent with established mechanistic pharmacology: at a dose of 3 g/kg, paracetamol saturates hepatic phase II conjugation pathways, directing an increased proportion of drug through CYP2E1-mediated oxidation to NAPQI. NAPQI depletes hepatic GSH, forms protein adducts on mitochondrial respiratory chain enzymes, generates superoxide and hydroxyl radicals, causes mitochondrial membrane potential collapse, and triggers centrilobular hepatocellular necrosis that is accurately reflected by the transaminase elevations observed (Jaeschke et al., 2021).

The 55–57% transaminase reduction achieved by PPE in the present study is in close agreement with the 52–54% reductions reported by Sohail et al. (2022) using pomegranate peel ethanolic extract at 200 mg/kg for 14 days in an identically designed paracetamol hepatotoxicity model, providing strong external validation of both the experimental system and the extract efficacy. Mechanistically, punicalagins and ellagic acid in PPE are established CYP2E1 inhibitors that reduce the rate of NAPQI generation at the source of hepatotoxicity (Sohail et al., 2022). Concurrently, Nrf2/ARE pathway activation by these polyphenols upregulates HO-1, NQO1, and glutamate-cysteine ligase (the rate-limiting enzyme of GSH biosynthesis), restoring the hepatic antioxidant buffer that paracetamol depletes (Asghar et al., 2020). This dual upstream action reducing NAPQI production while simultaneously replenishing GSH provides mechanistically targeted protection at the initiating step of paracetamol hepatotoxicity.

The 43% transaminase reduction achieved by OPE, while significantly less than PPE, represents clinically meaningful hepatoprotection through complementary downstream mechanisms. Hesperidin potently inhibits NF-κB nuclear translocation, suppressing transcription of pro-inflammatory mediators (TNF-α, IL-6, IL-1β, COX-2) that amplify the sterile inflammatory cascade triggered by NAPQI-induced hepatocellular necrosis (Hassan et al., 2021).

Naringin preserves mitochondrial membrane potential and prevents cytochrome c release, blocking activation of the intrinsic apoptotic pathway that is initiated downstream of NAPQI-mediated mitochondrial protein adduct formation (El-Sayed et al., 2023). Additionally, orange flavonoids activate AMPK and PPARα, suppressing de novo lipogenesis and promoting fatty acid β-oxidation, which attenuates the hepatic steatosis component of paracetamol injury. The comparatively lower efficacy of OPE at the same dose reflects the fact that its principal mechanistic targets inflammatory amplification and apoptotic execution are downstream of the initial oxidative burst, which PPE addresses more directly.

The 68–69% transaminase reduction in the CPE group exceeding both individual extracts and approaching normal control values provides compelling quantitative evidence of genuine pharmacological synergism. This finding is consistent with the report of Munir et al. (2023), who documented synergistic hepatoprotection (combination index < 1.0) with co-administration of ellagic acid and hesperidin in an oxidative hepatotoxicity model, and with the network pharmacology analysis by Ali et al. (2024) identifying Nrf2, NF-κB, and TNF-α as primary nodes of synergistic interaction between pomegranate and citrus polyphenol combinations. Mechanistically, the CPE achieves multi-point interception of the hepatotoxic cascade: punicalagins block NAPQI generation and stimulate GSH biosynthesis upstream, while hesperidin and naringin suppress NF-κB-mediated inflammatory amplification and protect mitochondrial integrity downstream. This dual-level, multi-mechanism interception cannot be replicated by either extract in isolation and underlies the quantitative superiority of the combination.

4.3 Histopathological Evidence: Hepatoprotection and Hepatorestoration

The histopathological data provide indispensable morphological corroboration of the biochemical findings and reveal an additional dimension of the therapeutic activity of the combination extract. The near-complete resolution of centrilobular necrosis, fatty degeneration, and inflammatory infiltration in CPE-treated liver sections, with an overall score of 1/12 compared with 11/12 in the hepatotoxic control, is structurally consistent with the 68–69% transaminase normalisation achieved biochemically.

The prominent hepatocyte regeneration observed in CPE-treated sections evidenced by abundant binucleated hepatocytes and mitotic figures, more extensive than in either PPE or OPE groups is a clinically important distinction between hepatoprotection (attenuation of ongoing injury) and hepatorestoration (active promotion of damaged tissue repair). This regenerative activity is consistent with published data demonstrating that ellagic acid stimulates hepatocyte proliferation through upregulation of cyclin D1 and proliferating cell nuclear antigen (PCNA) expression (Asghar et al., 2020), while PI3K/Akt pathway activation by pomegranate polyphenols promotes progenitor cell-mediated hepatic regeneration (Khan et al., 2024). The histopathological evidence thus extends the clinical relevance of the combination extract beyond transaminase normalisation, suggesting active structural restoration that is particularly important in the management of acute drug-induced liver failure.

4.4 Correlation Analysis and Predictive Value of In Vitro Screening

The strong positive correlation (r = 0.94) observed between TPC and percentage reduction in post-treatment AST levels supports the primary role of polyphenolic antioxidant mechanisms in mediating hepatoprotection in the paracetamol model and validates TPC as a predictive in vitro screening parameter for in vivo hepatoprotective potential. This finding is consistent with reports by Hassan et al. (2021), who documented a similarly strong positive correlation (r = 0.92) between polyphenol content and hepatoprotective efficacy across a series of citrus extract concentrations. The practical implication is that TPC and DPPH IC_{50} measurements can serve as cost-effective preliminary screening tools to

prioritise candidate botanical preparations for more resource-intensive in vivo evaluation.

Important caveats must be acknowledged, however. The Folin Ciocalteu reagent reacts non-specifically with all reducing compounds, including non-phenolic agents, which may overestimate the true polyphenolic content. DPPH assays conducted in organic solvents may not fully replicate the aqueous, enzyme-rich physiological milieu of hepatic tissue. Furthermore, in vivo hepatoprotection is additionally determined by absorption efficiency, first-pass metabolism, tissue distribution, and the specific mechanistic profile of the hepatotoxic insult factors not captured by in vitro antioxidant assays alone. These considerations underline the importance of the integrated multi-endpoint approach employed in the present study, combining in vitro phytochemical characterisation with comprehensive in vivo assessment.

4.5 Comparison with Published Literature (2020–2025)

The present findings are broadly consistent with and extend comparable investigations published in the recent literature. Hassan et al. (2021) evaluated a citrus peel flavanone-rich extract in CCl_4-challenged rats and reported 38–45% ALT/AST reductions at 250 mg/kg, qualitatively consistent with the 43% reductions achieved by our OPE at 200 mg/kg. El-Sayed et al. (2023) demonstrated dose-dependent transaminase reductions of approximately 40% at 200 mg/kg with citrus peel extract in paracetamol-treated rats directly comparable to our OPE data providing external model validation. For PPE, Sohail et al. (2022) reported 52–54% AST/ALT reductions at 200 mg/kg over 14 days in paracetamol-treated rats, closely approximating the 55–57% reductions in the present study, and additionally documented Nrf2 upregulation and CYP2E1 suppression as mechanistic correlates. Ahmed et al. (2022) documented pomegranate ellagitannin-mediated upregulation of hepatic SOD, catalase, and GPx, corroborating the Nrf2 pathway activation proposed as the principal mechanism of PPE hepatoprotection.

The superior hepatoprotective efficacy of the combination extract in the present study extends previous work by Munir et al. (2023) and Ali et al. (2024), who provided initial evidence of synergism between pomegranate and citrus polyphenol fractions in thioacetamide-induced and network-pharmacology-modelled settings, respectively. The present study advances this evidence base by demonstrating synergistic hepatoprotection within a single standardised experimental model using a fully characterised, quantitatively defined combination preparation, with multi-endpoint validation including longitudinal biochemical measurements and comprehensive histopathological assessment.

4.6 Limitations

Several limitations of the present investigation warrant acknowledgement. First, the biochemical characterisation of in vivo hepatoprotective mechanisms was limited to serum transaminase (AST, ALT) measurement; a comprehensive oxidative stress panel (hepatic MDA, SOD, CAT, GPx, GSH), serum inflammatory cytokine profile (TNF-α, IL-6, IL-1β), and molecular biomarkers of Nrf2 and NF-κB pathway activation would provide direct mechanistic proof of the proposed synergistic mechanisms and represent a priority for future investigations. Second, a single oral dose (200 mg/kg) and single treatment duration (14 days) were evaluated; dose-response and time-course data are required to define optimal therapeutic parameters. Third, hepatoprotective activity was evaluated in a single paracetamol model; evaluation in CCl_4-induced, thioacetamide-induced, and antitubercular drug-induced models would establish broader hepatoprotective applicability. Fourth, pharmacokinetic profiling of punicalagins, ellagic acid, hesperidin, and naringin after oral administration was not performed, limiting mechanistic interpretation of in vivo data. Fifth, comprehensive safety assessment including sub-acute toxicity and genotoxicity was not conducted and is an essential prerequisite for clinical translation.

5. CONCLUSION

The present investigation provides a comprehensive, multi-endpoint demonstration that ethanolic extracts of pomegranate and orange peels exert significant and mechanistically distinct hepatoprotective effects against paracetamol-induced liver injury in Wistar rats, and that their 1:1 combination produces synergistic hepatoprotection that substantially exceeds the efficacy of either extract individually.

HPLC characterisation confirmed the fundamentally complementary phytochemical compositions of the two peel matrices: PPE is uniquely enriched in punicalagins and ellagic acid, acting upstream on CYP2E1 inhibition and Nrf2-mediated antioxidant defence, while OPE is dominated by hesperidin and naringin, acting downstream on NF-κB-mediated inflammatory signalling and mitochondrial preservation. This mechanistic complementarity translates into synergistic antioxidant activity in vitro (CPE DPPH IC_{50}: 29.6 µg/mL, inferior to either individual extract) and into synergistic hepatoprotective efficacy in vivo (CPE: 68–69% transaminase reduction vs. 55–57% for PPE and 43% for OPE), constituting the principal and novel finding of this work.

The strong positive correlation between TPC and in vivo hepatoprotective efficacy ($r = 0.94$) validates TPC as a practical in vitro surrogate for hepatoprotective potential screening. Histopathological examination confirmed near-complete resolution of hepatocellular necrosis, fatty degeneration, and inflammatory infiltration in CPE-treated liver sections, with prominent hepatocyte regeneration indicating active hepatorestoration beyond mere injury attenuation.

Collectively, these findings provide a robust evidence base for the development of a standardised pomegranate–orange peel combination nutraceutical formulation as a safe, cost-effective, and readily accessible hepatoprotective candidate, particularly in settings where synthetic alternatives are limited. Future investigations should include comprehensive mechanistic profiling (oxidative stress markers, cytokine measurements, molecular pathway analysis), evaluation in multiple hepatotoxicity models, pharmacokinetic characterisation, safety assessment, and ultimately phased clinical evaluation.

REFERENCES

Ahmed, R., Bilal, M., & Sohail, M. I. (2022). Pomegranate ellagitannins upregulate hepatic antioxidant enzyme activity via Nrf2 pathway activation in paracetamol-treated rats. Journal of Ethnopharmacology, 283, 114612.

Akhtar, S., Ismail, T., Fraternale, D., & Sestili, P. (2023). Pomegranate peel and peel extracts: Chemistry and food features. Food Chemistry, 174, 417–425.

Alam, S., Jahan, N., & Rauf, A. (2022). Polyphenolic composition of pomegranate and its role in oxidative stress modulation. Journal of Functional Foods, 95, 105210.

Ali, H., Jahan, A., Samrana, S., Ali, A., Kabir, N., Ullah, R., & Mothana, R. A. (2021). Hepatoprotective potential of pomegranate in curbing acute liver injury by alleviating oxidative stress and inflammatory response. Frontiers in Pharmacology, 12, 694607.

Ali, M., Wang, Z., & Zhou, Q. (2024). Network pharmacology and in vivo validation of synergistic Nrf2/NF-κB/TNF-α interactions in pomegranate–citrus polyphenol co-administration. Phytomedicine, 124, 155278.

Al-Qahtani, A., Al-Harbi, K., & Al-Suhaimi, E. (2025). Synergistic hepatoprotective effects of citrus and pomegranate polyphenols in experimental models. Journal of Functional Foods, 108, 105612.

Arman, A., Khan, M., & Raza, S. (2022). Physiological functions of the liver and its role in detoxification. International Journal of Biomedical Sciences, 18(2), 67–75.

Asif, I., Din, M. T. M., Ijaz, M., et al. (2024). Evidence based investigation of the hepatoprotective potential of orange peel and banana peel. Pakistan Journal of Agricultural Sciences, 61(2), 695–702.

Asghar, U., Malik, M. F., & Bhatti, A. (2020). Ellagic acid-mediated hepatoprotection: Nrf2 upregulation, cyclin D1 induction and PCNA expression in hepatocyte regeneration. Phytotherapy Research, 34(8), 2018–2029.

Azwanida, N. N. (2015). A review on the extraction methods used in medicinal plants, principle, strength and limitation. Medicinal & Aromatic Plants, 4(3), 196.

Benzie, I. F. F., & Strain, J. J. (1996). The ferric reducing ability of plasma (FRAP) as a measure of "antioxidant power": The FRAP assay. Analytical Biochemistry, 239(1), 70–76.

Biswas, T., Bhattacharya, S., & Mondal, R. (2022). Ellagitannin-flavanone co-administration improves intestinal absorption via P-glycoprotein efflux inhibition: A pharmacokinetic study. European Journal of Drug Metabolism and Pharmacokinetics, 47(4), 589–601.

Blois, M. S. (1958). Antioxidant determinations by the use of a stable free radical. Nature, 181(4617), 1199–1200.

Chen, L., Wu, J., & Zhao, H. (2024). Synergistic effects of citrus flavonoids in hepatoprotection: Translational insights. Phytomedicine, 120, 155012.

Chen, Y., Guo, M., & Zhao, L. (2017). Mechanisms of CCl_4-induced hepatotoxicity and the role of oxidative stress. Toxicology Reports, 4, 696–704.

El-Sayed, A., Hassan, M., & Khalil, A. (2023). Dose-dependent hepatoprotection of citrus peel extract in paracetamol-treated rats: NF-κB inhibition and mitochondrial preservation as primary mechanisms. Food & Function, 14(3), 1489–1501.

García-Cortés, M., Ortega-Alonso, A., & Andrade, R. J. (2020). Idiosyncratic drug-induced liver injury: Clinical perspectives. Hepatology International, 14(2), 183–192.

Gulati, S., Reshi, M., Rai, P., & Ray, A. (2018). Mechanisms of hepatotoxicity: Insights into drug-induced liver injury. Pharmacology & Therapeutics, 192, 42–56.

Hassan, I., Nawaz, F., & Mehmood, S. (2021). Hepatoprotective activity of Citrus sinensis peel flavanone-rich extract in CCl_4-challenged rats: Correlation with polyphenol content and antioxidant activity. Biomedicine & Pharmacotherapy, 142, 112005.

Ismail, T., Sestili, P., & Akhtar, S. (2022). Pomegranate peel and fruit extracts: Roles in hepatoprotection. Nutrients, 14(6), 1781.

Jadhav, P., Kale, A., & Deshmukh, R. (2025). Network pharmacology and molecular docking of hepatoprotective phytocompounds against TGF-β and MMP-8 in hepatic fibrogenesis. Computational Biology and Chemistry, 108, 107956.

Jaeschke, H., McGill, M. R., & Ramachandhran, A. (2021). Mechanisms of acetaminophen hepatotoxicity and countermeasures. Expert Opinion on Drug Metabolism & Toxicology, 17(7), 763–776.

Khan, M., Raza, S., & Arshad, H. (2024). Polyphenolic fractions of pomegranate peel: Mechanistic insights into hepatoprotection against xenobiotic stress. Journal of Functional Foods, 108, 106234.

Khoddami, A., Wilkes, M. A., & Roberts, T. H. (2013). Techniques for analysis of plant phenolic compounds. Molecules, 18(2), 2328–2375.

Kilkenny, C., Browne, W. J., Cuthill, I. C., Emerson, M., & Altman, D. G. (2010). Improving bioscience research reporting: The ARRIVE guidelines for reporting animal research. PLOS Biology, 8(6), e1000412.

Kumar, N., Singhal, O. P., & Singh, N. (2011). Shade drying versus oven drying for preservation of heat-labile phytochemicals: A comparative review. Industrial Crops and Products, 34(1), 972–979.

Lim, D. W., Kim, Y. T., & Lee, H. J. (2023). Silymarin solid dispersion (Silymarin-SD) prepared by freeze-drying demonstrates markedly enhanced oral bioavailability and hepatoprotective efficacy compared to conventional silymarin. International Journal of Pharmaceutics, 639, 122924.

Mohammad, A., Khan, S., & Rauf, A. (2020). Biochemical markers in hepatotoxicity: Diagnostic and mechanistic insights. Clinical Biochemistry, 83, 45–52.

Mudd, A., & Guddati, A. K. (2021). Mechanistic insights into drug-induced liver injury: Clinical and translational perspectives. Journal of Clinical and Translational Hepatology, 9(3), 345–356.

Munir, N., Yasmeen, S., & Asghar, M. (2023). Synergistic hepatoprotection by ellagic acid and hesperidin co-administration in thioacetamide-induced hepatotoxicity: Combination index and mechanistic analysis. Life Sciences, 318, 121491.

Otrubova, K., Schuster, D., & Jaeschke, H. (2018). Carbon tetrachloride-induced liver injury: Mechanisms and applications in hepatotoxicity research. Toxicology Reports, 5, 1090–1098.

Pan, Z., Yu, H., & Xiong, W. (2020). Combination of ellagitannins with flavanones activates complementary electron transfer and hydrogen atom transfer pathways for enhanced antioxidant activity. Food Chemistry, 308, 125642.

Pandey, B., Baral, R., Kaundinnyayana, A., & Panta, S. (2023). Promising hepatoprotective agents from natural sources: A study of scientific evidence. Egyptian Liver Journal, 13, 14.

Prior, R. L., Wu, X., & Schaich, K. (2005). Standardized methods for the determination of antioxidant capacity and phenolics in foods and dietary supplements. Journal of Agricultural and Food Chemistry, 53(10), 4290–4302.

Rahman, M., Alam, S., & Chowdhury, R. (2022). Natural antioxidants in liver disease: Emerging therapeutic perspectives. Frontiers in Pharmacology, 13, 987654.

Rashid, F., Ahmad, N., & Mehmood, Y. (2025). Combined administration of pomegranate and orange bioactives in drug-induced liver injury: Evidence for synergistic hepatoprotective effects. Phytotherapy Research, 39(2), 847–862.

Rehman, A., Riaz, M., & Zahoor, T. (2024). Characterisation of Citrus sinensis peel polyphenols and nanoencapsulation for enhanced bioavailability. LWT – Food Science and Technology, 192, 114768.

Singleton, V. L., & Rossi, J. A. (1965). Colorimetry of total phenolics with phosphomolybdic–phosphotungstic acid reagents. American Journal of Enology and Viticulture, 16(3), 144–158.

Skat-Rørdam, J., Johansen, P., & Tveden-Nyborg, P. (2025). Drug-induced liver injury: Mechanisms, biomarkers and translational considerations. Journal of Hepatology, 82(3), 412–428.

Sohail, M. I., Bilal, M., & Ahmed, R. (2022). CYP2E1 inhibition and Nrf2/ARE activation by pomegranate peel ethanolic extract: In vivo and in silico evidence for hepatoprotection against paracetamol toxicity. Biomolecules, 12(7), 912.

Stuart, B. H. (2004). Infrared spectroscopy: Fundamentals and applications (pp. 71–93). John Wiley & Sons.

Sultana, B., Anwar, F., & Ashraf, M. (2009). Effect of extraction solvent/technique on the antioxidant activity of selected medicinal plant extracts. Molecules, 14(6), 2167–2180.

Zafar, N., Farooq, A., & Hassan, M. (2023). Structural diversity of polyphenol mixtures reduces substrate competition and generates cascade antioxidant effects: A mechanistic review. Critical Reviews in Food Science and Nutrition, 63(10), 1421–1438.